

SYNTHESIS, CHARACTERIZATION OF POLYVINYL ALCOHOL-CHITOSAN-ZNO/CUO NANOPARTICLES FILM AND ITS BIOLOGICAL EVALUATION AS AN ANTIBACTERIAL AGENT OF *Staphylococcus aureus*

AHMAD FATONI^{1*}, MAUIZATUL HASANAH¹, LASMARYNA SIRUMAPEA¹, ANNISA DEFANIE PUTRI¹, KHOIRUNNISA SARI¹, RESTU DWI KHAIRANI¹, AND NURLISA HIDAYATI²

¹Department of Pharmacy, Bhakti Pertiwi College of Pharmacy,
Palembang, South Sumatera, Indonesia

²Department of Chemistry, Faculty of Mathematics and Natural Sciences,
Sriwijaya University, Indralaya Ogan Ilir South Sumatera, Indonesia

*Corresponding author email: tonistifbp@gmail.com

Article Information

Received: Mar 22, 2023
Revised: Jun 13, 2023
Accepted: Jun 21, 2023
Published: Jun 30, 2023

DOI:
10.15575/ak.v10i1.24725

Keywords:
PVA-chitosan-
ZnO/CuO; nanoparticles;
film;
characterization;
Staphylococcus aureus.

Abstract

The polyvinyl alcohol-chitosan-ZnO/CuO nanoparticles film was researched. Synthesis, characterization, and its biological evaluation as an antibacterial of *Staphylococcus aureus* were the aims of this research. The biosynthesis of ZnO, CuO, and ZnO/CuO nanoparticles was done using the biological method. The polyvinyl alcohol-chitosan-ZnO/CuO nanoparticles film was synthesized using the casting method. All the products were characterized by FTIR spectroscopy, X-ray diffraction, and Scanning Electron Microscope (SEM). Polyvinyl alcohol-chitosan-ZnO/CuO nanoparticles film as a paper disk for the evaluation as an antibacterial agent through the agar disk diffusion method. The absorption bands of ZnO, CuO, and ZnO/CuO nanoparticles can be observed at 318, 274, and 252 nm, respectively. The peaks at wavenumbers 433-673 and 619 cm⁻¹ were Zn-O and Cu-O groups, respectively. The Zn-O and Cu-O groups at ZnO/CuO nanoparticles can be observed at 474 and 619 cm⁻¹. The appearance of Zn-O and Cu-O groups at film PVA-chitosan-ZnO/CuO nanoparticles indicates the wavenumber between 433 and 673 cm⁻¹. The physical structure of ZnO, CuO, and ZnO/CuO nanoparticles is crystalline form. The crystallite size of ZnO, CuO, and ZnO/CuO nanoparticles was estimated at 1.0572, 6.6315, and 2.3333 nm respectively. The physical structure of film PVA-chitosan-ZnO/CuO nanoparticles is amorphous. The surface morphology of films C, D, and E was affected by the addition of chitosan and ZnO/CuO nanoparticles. The film of PVA-chitosan-ZnO/CuO nanoparticles (C, D and E) can act as an antibacterial agent of *Staphylococcus aureus*. The inhibition zone of film D is higher than A, B, C, and E.

INTRODUCTION

There are three methods in the synthesis process of metal nanoparticles. Physical, chemical, and biological methods are the major ones in this synthesis [1]. Previous literature [2] has stated that physical, chemical, and biological methods have their advantages and disadvantages, respectively. The advantages and disadvantages of the physical method are the absence of toxic chemicals and the requirement of expensive instrumentation in the synthesis process, respectively. The chemical method has advantages such as high yield, but the disadvantage of this synthesis method is the use of toxic chemicals. The last method is the biological method, where the synthesis process is easy but controlling the size of metal nanoparticles is challenging. The biological method has a challenge in the synthesis process such as the

effect of pH, the concentration of reactant, reaction time, and temperature [3]. On the contrary, despite the challenges associated with the biological method, researchers have chosen this method because it is easy and cheap [4]. Plants (leaves etc), algae, bacteria, yeast, and fungus serve as the basic material in the biosynthesis of metal oxide nanoparticles through the biological method [5] and it was explored by previous literature [6] [7] [8] [9] [10]. However, the biosynthesis of these nanoparticles using extracts from plants is easier than with algae, bacteria, yeast, and fungus. The biosynthesis of metal oxide nanoparticles using algae, bacteria, yeast, and fungus requires specific conditions [11].

The common solvent for the biosynthesis process is a non-alcoholic or alcoholic solvent based on the polarity index. Non-alcoholic solvents (water) and alcoholic solvents (ethanol)

have polarity indices of 9 and 5.2 [12], respectively. However, ethanol solvent is a universal solvent and demonstrates strength in the extraction process. A hydroxyl group and an alkyl group in the ethanol solvent affect the extraction process. The polar or non-polar properties of secondary metabolites in the plant can be extracted and dissolved by an ethanol solvent [13]. The ethanolic extract of the plant serves as the medium in the biosynthesis of metal oxide nanoparticles [14] [15] [16] [17]. The plant extract can be used as a medium for the biosynthesis of double metal oxide nanoparticles (bimetallic) as well as ZnO/CuO nanoparticles [18] [19] [20], and the product of ZnO/CuO nanoparticles can act as an antibacterial [21]. ZnO/CuO nanoparticles have a synergistic effect, on the other hand, the multifunctional bimetallic nanoparticles can be used in various fields [22].

Chitosan is derived from chitin. The advantages of chitosan are its non-toxicity and safety for use [23] [24]. The biological properties of chitosan include its antimicrobial activity [25]. To increase the film formation, chitosan can be mixed with polyvinyl alcohol (PVA). PVA is classified as a synthetic polymer and can be used as a film-forming agent [26] [27] [28], as well as easily forming hydrogels [29]. Furthermore, it enhances the chemical properties of chitosan [30]. In contrast, chitosan as an organic material, can be used as a supporting material to increase the effectiveness and properties of bimetallic nanoparticles [22].

We biosynthesized bimetallic nanoparticles (ZnO/CuO nanoparticles) following a procedure proposed by previous literature [18], with a slight modification. Here, we employed the casting method to synthesize the PVA-chitosan-ZnO/CuO nanoparticles film. The resulting film was used to inhibit the growth of the *Staphylococcus aureus* bacteria. The PVA-chitosan-ZnO/CuO nanoparticles film was characterized by various techniques such as FTIR, XRD, and SEM. The biosynthesis (double metal oxide nanoparticles), as well as synthesis (PVA-chitosan-ZnO/CuO nanoparticles film), are discussed.

EXPERIMENT

Material

NaOH, CH₃COOH, Zn(CH₃COO)₂ · 2H₂O, CuSO₄ · 5H₂O, CH₃CH₂OH, Polyvinyl alcohol, and nutrient agar were purchased from PT. Merck. Chitosan (DD 87%) was from CV. Ocean Fresh

Bandung, West Java, Indonesia. Aquadest and *Staphylococcus aureus* were obtained from our laboratory (Microbiology Laboratory). Guava seed leaves (*Psidium guajava* L) were sourced from Palembang.

Instrumentation

The Instruments used for characterization were as follows: *FTIR Spectrophotometer* (Shimadzu Prestige-21) for functional group analysis. *X-Ray diffraction* (XRD, Shimadzu 6000) for physical structure analysis. *UV-Vis Spectrophotometer* (Genesys 150 Thermo Scientific) for the analysis of metal nanoparticle wavelengths and *Scanning Electron Microscopy* (SEM, JEOL JSM 6510 LA) for surface morphology analysis

Procedure

Maceration process of leaves guava seed

The ethanolic extract of leaves guava seed was prepared using the maceration method, as proposed by previous literature [16] with slight modification. Dried guava seed leaves (25 g) were soaked in ethanol 70 % (v/v, 250 mL) for 24 hours in a maceration bottle. After 24 hours, the filtrate was separated, and it was collected in a clean bottle, and stored at room temperature (filtrate I). The residue was macerated again with 250 mL ethanol 70 % (v/v) (24 h). The filtrate was filtered, and the filtrate was collected and merged with filtrate I. All filtrate was stored a room temperature for further experiment.

Biosynthesis of metal oxide nanoparticles [18]

The ethanolic extract of guava seed leaves (75 mL) in a beaker glass 250 mL was added to the solution of zinc acetate dihydrate (0.5500 g, 25 mL). The process of biosynthesis was done on a hot plate (80°C) with continuous stirring (60 minutes). After 60 minutes, sodium hydroxide solution (0.1 M, 10 mL) was added to this mixture and stirred continuously up to pH 10. The mixture was stored for one night until the precipitation appeared. The filtrate and residue (ZnO nanoparticles) were separated, and ZnO nanoparticles were washed with aquadest (15 ml) and absolute ethanol (15 mL). The product of ZnO nanoparticles was dried in the oven (60° C) until dry. The same procedure was used to prepare CuO and ZnO/CuO nanoparticles and summarized in **Table 1**.

Table 1. The materials in the biosynthesis of metal oxide nanoparticles.

No	The ethanolic extract of guava seed leaves (mL)	Zinc acetate dihydrate (g)	copper sulfate pentahydrate (g)	Aquadest (mL)	sodium hydroxide solution (M, mL)	The name of product
1	75	0.5500	-	25	0.1, 10	ZnO nanoparticles
2	75	-	0.6250	25	0.1, 13	CuO nanoparticles
3	75	0.5500	0.6250	25	0.1, 13	ZnO/CuO nanoparticles

Synthesis of the PVA-chitosan-bimetallic oxide nanoparticles film

PVA-chitosan-ZnO/CuO nanoparticles film (film C) was synthesized using an earlier procedure [31] with slight modification. Chitosan solution in 250 mL of beaker glass (0.1 g of chitosan powder and 10 mL of acetic acid solution 1% v/v). ZnO/CuO nanoparticles (0.1 g) were added to the chitosan solution by continuously

stirring (room temperature, 1 h). Then the PVA solution (2.5 % (w/v), 10 mL) was added to this mixture. All mixture was stirred continuously for 30 minutes at room temperature. The PVA-chitosan-ZnO/CuO nanoparticles were poured into a petri dish until dry at room temperature. The film D and E were prepared with the same procedure. Film A and B were prepared by adding PVA solution and metal oxide nanoparticles without chitosan as explained in **Table 2**.

Table 2. The composition of chitosan, ZnO, CuO, and ZnO/CuO nanoparticles in the synthesis of all film

No	Film	The comparison between chitosan, ZnO, CuO, and ZnO/CuO nanoparticles		
		chitosan (g)	PVA 2.5% (w/v), mL	mass (g) of metal oxide nanoparticle
1	A	-	10	0.1 (ZnO nanoparticles)
2	B	-	10	0.1 (CuO nanoparticles)
3	C	0.1	10	0.1 (ZnO/CuO nanoparticles)
4	D	0.1	10	0.2 (ZnO/CuO nanoparticles)
5	E	0.2	10	0.1 (ZnO/CuO nanoparticles)

The antibacterial procedure of the film PVA-chitosan-metal oxide nanoparticles

Three Petri plates were used in this evaluation. The antibacterial agent of PVA-chitosan-metal oxide nanoparticles film was evaluated by the agar disc diffusion method and the antibacterial procedure was adopted from our studies [32]. The procedure from Isnaeni *et al.* [33] was used to prepare the inoculum of the bacterial suspension. The film A, B, C, D, and E (± 6 mm in diameter respectively) was pasted in the second layer of nutrient agar. The second layer of nutrient agar contained the bacterial suspension. Incubation process at 37°C for 24 h. After 24 hours, the inhibition zone was observed.

RESULT AND DISCUSSION

Biosynthesis of Metal Oxide Nanoparticles, Synthesis of the PVA-Chitosan-Bimetallic Oxide Nanoparticles Film, and The Products

The process of biosynthesis of nanoparticles was described in **Figure 1** as reported by Fouda et al [18]. The materials were used in the biosynthesis of metal oxide nanoparticles such as Zn²⁺, Cu²⁺ ion, media of biosynthesis (ethanolic extract), and NaOH solution. Ethanolic extract of guava seed leaves are containing active biomolecules [34]. The biomolecules were activated at pH 10 and at this pH, the biomolecules will increase them. A previous paper [35] has explained that at alkaline pH, the electrical charges of biomolecules can be converted into capping and stabilizing agents.

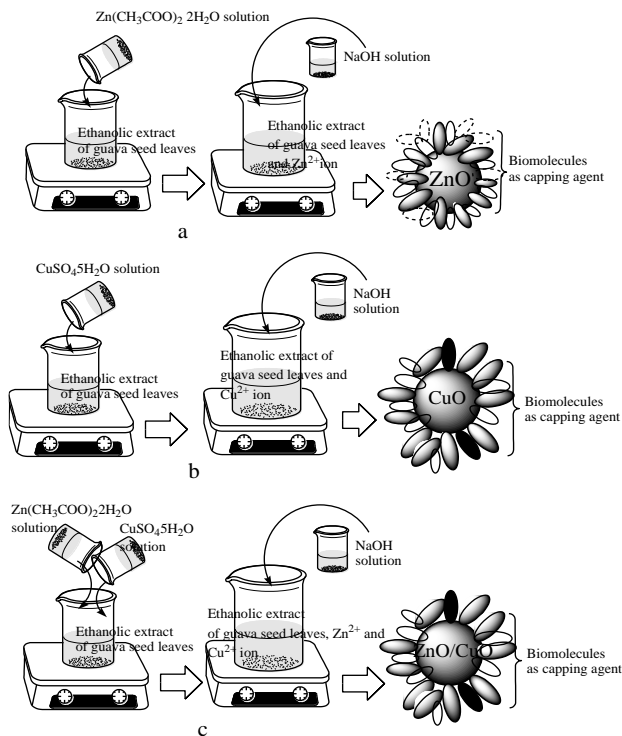


Figure 1. Biosynthesis process of ZnO nanoparticles (a), CuO nanoparticles (b), and ZnO/CuO nanoparticles (c) [18].

Figure 2 and **3** shows the product of biosynthesis of ZnO, CuO, and ZnO/CuO nanoparticles and the product of the film respectively.

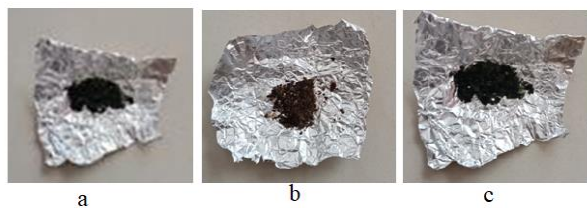


Figure 2. ZnO nanoparticles (a), CuO nanoparticles (b), and ZnO/CuO nanoparticles (c).

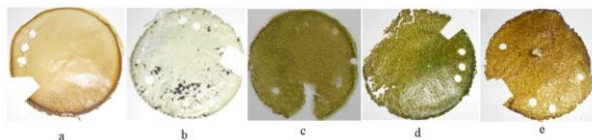


Figure 3. The photograph of film PVA-ZnO nanoparticles (a, film A), PVA-CuO nanoparticles (b, film B), PVA-chitosan-ZnO/CuO nanoparticles (c, film C), PVA-chitosan-ZnO/CuO nanoparticles (d, film D) and PVA-chitosan-ZnO/CuO nanoparticles (e, film E).

Characterization of Metal Oxide Nanoparticles by UV-Vis Spectrophotometer

The UV-visible spectra of ZnO, CuO, and ZnO/CuO nanoparticles were analyzed in the

range of 200-800 nm and shown in **Figure 4**. The specific absorbance for ZnO, CuO, and ZnO/CuO nanoparticles were synthesized by using the ethanolic extract of guava seed leaves at 318, 274, and 252 wavelengths (nm), respectively. For ZnO nanoparticles, the absorption bands at 318 nm confirmed the existence of ZnO nanoparticles [7]. At this peak, there is a transfer of electrons from the valence band (VB) to the conduction band (CB) [8].

The absorption band at 274 nm for CuO nanoparticles has similarities with previous literature [36] due to the core electrons of the CuO nanoparticles running into the interband transition [37]. The absorption peak for ZnO/CuO nanoparticles at 252 nm and its appearance in a single absorption band [38].

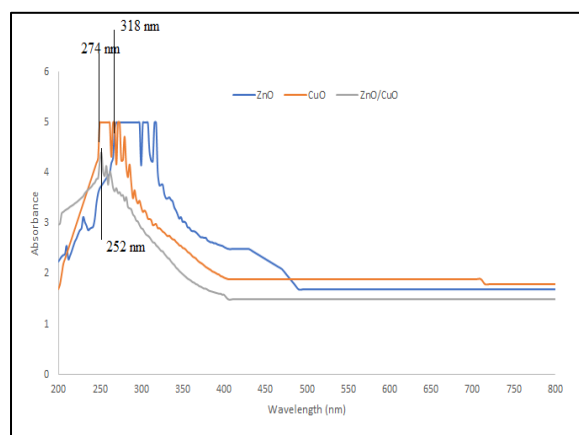


Figure 4. UV-Vis spectra of ZnO, CuO, and ZnO/CuO nanoparticles.

Characterization of Metal Oxide Nanoparticles and All Films by FTIR Spectrophotometer

The FTIR spectra of ZnO, CuO, and ZnO/CuO nanoparticles as seen in **Figure 5**. In **Figure 5** a, b, and c, the O-H and N-H groups (stretching vibration) can be observed in the wavenumber at 3423-3448 cm⁻¹ [39]. This wavenumber appeared from a secondary metabolite as a bioactive compound from the ethanolic extract of guava seed leaves. The group of C=C, C=N, and C=O can be observed at 929-1620 cm⁻¹. The band below 1000 cm⁻¹ is the characteristic of metal oxide absorption because of interatomic vibration [39]. The Cu-O group (stretching vibration) appeared at 619 cm⁻¹ [40],[41],[42]. The band at 433-673 cm⁻¹ is the stretching vibration Zn-O group [9],[43],[44] and the Zn-O/Cu-O groups (stretching vibration) appeared at 474 and 619 cm⁻¹ [18].

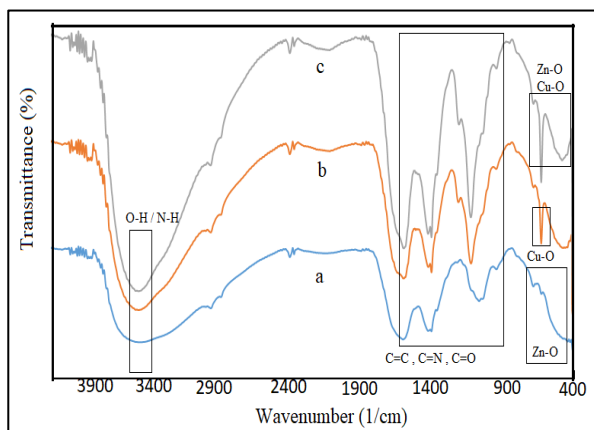


Figure 5. FTIR spectra of ZnO nanoparticles (a), CuO nanoparticles (b), and ZnO/CuO nanoparticles (c).

Figure 6 shows the FTIR spectral characteristic of PVA film, films A and B. The FTIR spectra of pure PVA film (Figure 6 a) showed -OH (stretching, 3410 cm^{-1}), -CH_2 (asymmetric, 2941 cm^{-1}), -CH_2 (symmetric stretching, 2908 cm^{-1}), C=O (stretching in the acetate group, 1720 cm^{-1}), -CH_2 (stretching, 1330 cm^{-1}), C-H (wagging, 1240 cm^{-1}), C-O (stretching of an acetyl group, 1097 cm^{-1}) and C-C group (850 cm^{-1}) [45]. The FTIR spectra of the PVA-ZnO nanoparticles film (Figure 6b) and PVA-CuO nanoparticles (Figure 6c) showed that the stretching vibration of the OH group shifted to a higher wave number at 3450 cm^{-1} . The band at $468\text{-}675\text{ cm}^{-1}$ in Figure 6b showed that the Zn-O group appeared in this spectra. The Cu-O group was observed at 619 cm^{-1} (Fig. 6 c). Kumaraswamy et al [46] reported the shift in wave number, a new peak can be observed, and the intensities of the peak in the FTIR spectra between Figure 6a and 6b, c showed a specific interaction between ZnO or CuO nanoparticles and a functional group of PVA.

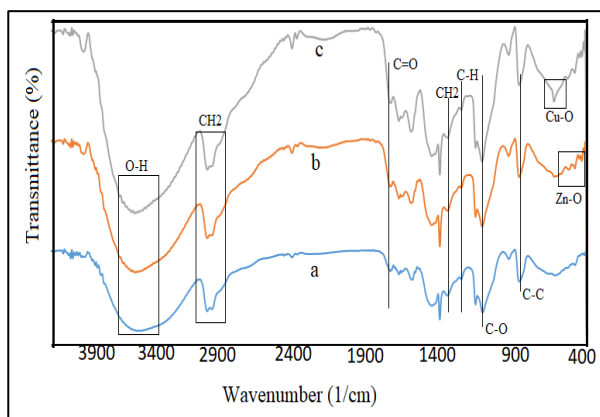


Figure 6. FTIR spectrum profile of PVA film (a), film of PVA-ZnO nanoparticles (b, film A), and PVA-CuO nanoparticles (c, film B).

The FTIR spectra of chitosan film, PVA film, film C, D and E as seen in **Figure 7**. Chitosan film (Figure 7a) showed bands at 3448 cm^{-1} (stretching vibration of O-H/N-H groups), 2920 cm^{-1} (stretching vibration of C-H groups), 1654 cm^{-1} (amide-I groups) and 1598 cm^{-1} (amide-II groups) [47]. The bands at FTIR spectra of PVA film (Figure 7b) were explained above. The wave number in the FTIR spectra of films C, D, and E (Figure 7c-e) has a wave number at 3429 , 3441 , and 3446 cm^{-1} respectively. The bands are the overlap of the stretching vibration of -NH and -OH groups from chitosan and PVA but all these bands are lower band than the band of stretching vibration of -NH and -OH groups chitosan film (3448 cm^{-1}) and higher than stretching vibration of -OH groups PVA film (3410 cm^{-1}). The functional groups of chitosan (-NH_2 and -OH) react with the functional groups of PVA (-OH) to form a hydrogen bonding and it can change this wave number [48],[49]. On the other hand, the peaks at amide-I of PVA-chitosan-ZnO/CuO nanoparticles film (C, D, E) shifted to lower wavenumber (1654 to $1587\text{-}1629\text{ cm}^{-1}$). The change in the wavenumber shows the interaction of reactive functional groups (-NH , -OH), and amide-I groups of chitosan with ZnO or CuO nanoparticles through a hydrogen bond [50] [51] and illustrated in **Figure 8**.

The FTIR spectra of C, D, and E films have differences with the FTIR spectra of chitosan and PVA, the bands at C, D, and E films, were observed at wavenumbers 617 , 615 , and 617 cm^{-1} respectively. Previous literature reported that the band between 433 and 673 cm^{-1} is the stretching vibration of the Zn-O or Cu-O group [9],[40],[41],[42],[43],[44] and the presence of Zn-O or Cu-O group was confirmed in this FTIR spectra of film C, D, and E.

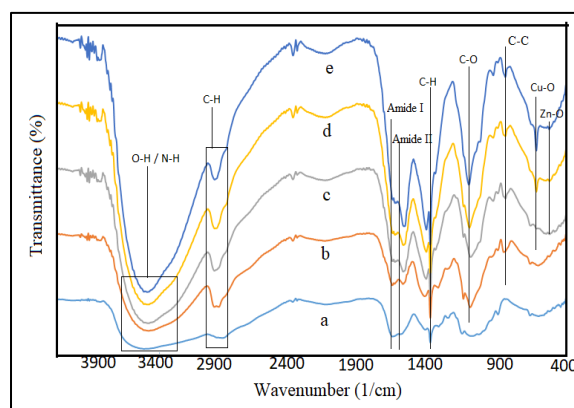


Figure 7. FTIR spectra of chitosan (a), PVA (b), film of PVA-chitosan-ZnO/CuO nanoparticles (c, film C), (film D, d) and (film E, e).

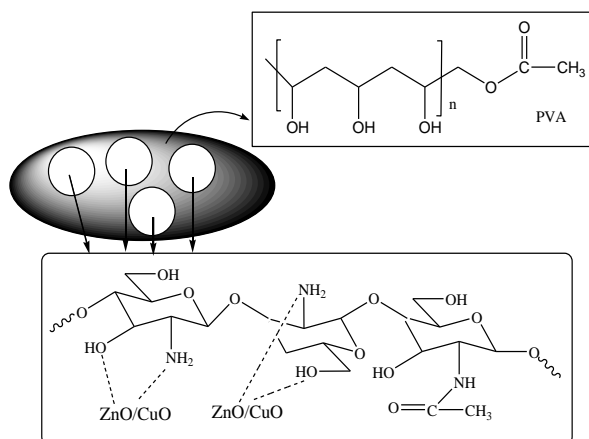


Figure 8. Illustration of chemical interaction between chitosan and ZnO/CuO nanoparticles [51].

Characterization of Metal Oxide Nanoparticles and All Films by XRD

The diffractogram of ZnO, CuO, and ZnO/CuO nanoparticles is seen in **Figure 9**.

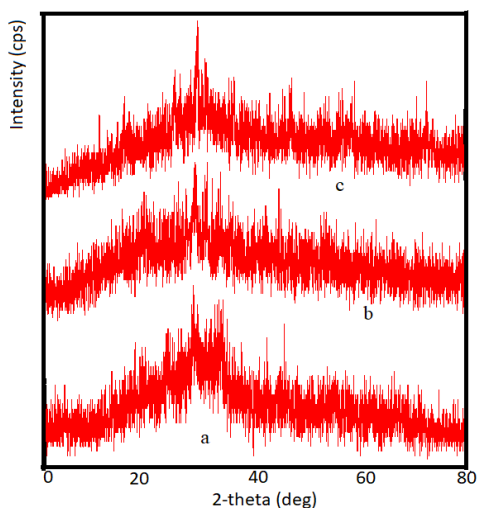


Figure 9. Diffractogram of ZnO nanoparticles (a), CuO nanoparticles (b), and ZnO/CuO nanoparticles (c).

The diffraction peaks from ZnO nanoparticles (Figure 9 a) with $2\theta = 23.7^\circ$, 31.46° , and 36.40° . These peaks can be connected to the crystal plans of (100) and (101) [52] and they have been used to estimate the average crystalline size. In the diffractogram of CuO nanoparticles (Figure 9 b), the diffraction peaks appeared at $2\theta = 31.56^\circ$ as a high-intensity peak [53]. The diffractogram ZnO/CuO nanoparticles (Figure 9c) at $2\theta = 28.31^\circ$, 32.59° and 59.98° [53]. The high-intensity peaks at $2\theta = 32.59^\circ$ are the peaks of CuO nanoparticles. The crystallite size of nanoparticles is calculated by Debye Scherrer's formula [54] as in equation 1.

$$D = (0.9.\lambda / \beta.\cos \theta) \quad (1)$$

D , λ , β , and θ are the crystallite size (nm), the wavelength of the X-ray used, the full width at half maximum (FWHM), and Bragg's angle respectively. The crystallite size of the biosynthesized ZnO, CuO, and ZnO/CuO nanoparticles was estimated at 1.0572, 6.6315, and 2.3333 nm, respectively.

All these sharp narrow peaks at the diffractogram of ZnO, CuO, and ZnO/CuO nanoparticles are indicated that the biosynthesis of ZnO, CuO, and ZnO/CuO nanoparticles is crystalline form. The description of the physical structure of films C, D, and E can be seen in **Figure 10**.

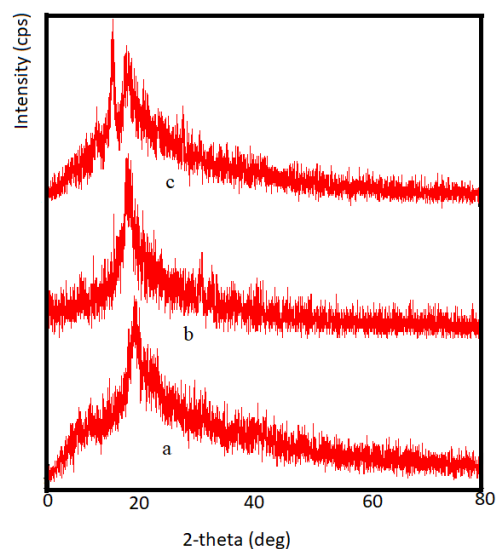


Figure 10. Diffractogram of film C (a), D (b) and E (c).

The XRD pattern of film C (Figure 10a) shows the peak at $2\theta = 10.50^\circ$, 19.65° , 25.50° and 70.60° . The peak at $2\theta = 10.50^\circ$ and 19.65° can be indicated as an amorphous phase of chitosan-PVA [46],[49]. The peaks of ZnO, and CuO nanoparticles can be observed at $2\theta = 25.50^\circ$ and 70.60° [47],[55] and the presence of ZnO or CuO nanoparticles in the PVA-chitosan network although the peak intensity of the ZnO or CuO nanoparticles is low due to the less concentration of ZnO or CuO nanoparticles. The peaks appeared at $2\theta = 10.40^\circ$, 18.83° and 25.73° was film D (Figure 10b), and in film E, the peaks appeared at $2\theta = 14.01^\circ$ and 16.91° (Figure 10c). Compared to the crystallite size of ZnO/CuO nanoparticles, the crystallite size of film PVA-chitosan-ZnO/CuO nanoparticles (film E) was 1 nm and there is a reduction to 1.3333 nm. All diffractogram in Figure 10 has an amorphous

structure. The chemical interactions between the OH and NH groups of the chitosan/PVA film and ZnO/CuO nanoparticles can change the physical structure [50],[51]. These interactions reduce the intra- and intermolecular hydrogen bond lengths and are observed in the FTIR spectra above.

Characterization of Metal Oxide Nanoparticles and All Films by SEM

The SEM images of ZnO, CuO, and ZnO/CuO nanoparticles are shown in **Figure 11**. The morphological study of ZnO nanoparticles shows that these nanoparticles have irregular morphology (Figure 11a). CuO nanoparticles have agglomerate based on the SEM images (Figure 11b) and the SEM images of ZnO-CuO nanoparticles showed the agglomeration of these bimetallic nanoparticles (Figure 11c).

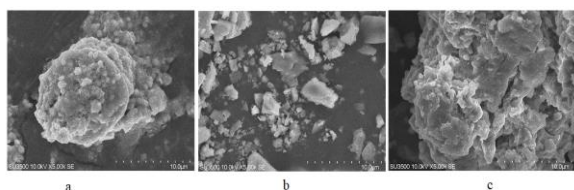


Figure 11. SEM micrographs of ZnO (a), CuO (b), and ZnO/CuO nanoparticles (c).

The SEM images of films C, D, and E are displayed in **Figure 12**. Figure 12a shows the synthesis of film C from the mixture of 0.1 g (ZnO/CuO nanoparticles), 10 mL (PVA 2.5%), and 0.1 g (chitosan) caused the surface morphology of film C to become rough, have a cavity and fracture. The surface morphology of Film D (the amount of chitosan is twice that of ZnO/CuO nanoparticles) is different than film C and E. The surface morphology of film D was less homogeneous causing the high concentration of chitosan [56]. The amount of ZnO/CuO nanoparticles is twice that of chitosan at film E, the fracture surface is seen the film E (Figure 12c). The fracture surface was caused by the binding effect between metal nanoparticles and chitosan structure as reported by Susilowati et al [57].

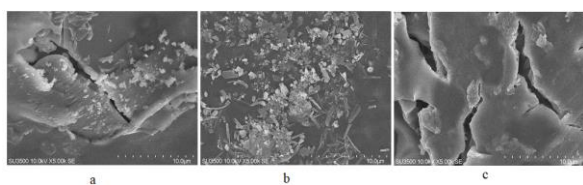


Figure 12. SEM micrographs of film C (a), film D (b), and film E (c).

Evaluation of All Films as Antibacterial

The antibacterial effect of all films was studied and seen in **Figure 13**. The calculation result of the inhibition zone is displayed in **Table 3**.

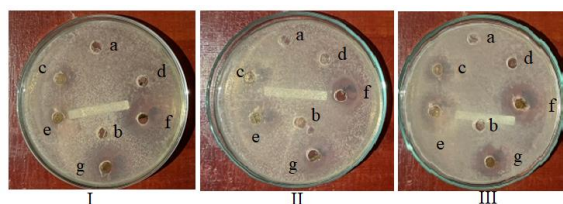


Figure 13. The inhibition zone of film of PVA (a), chitosan (b), PVA-ZnO nanoparticles (film A, c), PVA-CuO nanoparticles (film B, d), Film C (e), film D (f), and film E (g).

Table 3 showed the average inhibition zone of films C, D, and E is higher than films A and B. The addition of bimetallic nanoparticles (ZnO or CuO nanoparticles) and chitosan resulted in better antibacterial properties of films C, D, and E against *Staphylococcus aureus* bacteria. An antibacterial of chitosan through the penetration of chitosan structure into the microorganisms' nuclei and the electrostatic forces [58]. The electrostatic forces can be defined as the positive charge in the chitosan structure (NH_3^+ groups) that can bond with the negative charge of the bacterial cell membrane.

Table 3. The evaluation of all films as antibacterial.

Film	Zone of inhibition formed (mm)			Average \pm SD
	Petri plate I	Petri plate II	Petri plate III	
PVA	5.76	5.86	5.86	5.82 \pm 0.05
Chitosan	6.56	6.46	6.43	6.48 \pm 0.06
A	10.01	14.23	9.88	11.37 \pm 2.47
B	6.70	6.81	7.96	7.15 \pm 0.69
C	11.93	14.95	10.16	12.34 \pm 2.42
D	14.28	19.90	17.31	17.16 \pm 2.81
E	12.10	17.26	11.55	13.63 \pm 3.14

ZnO or CuO nanoparticles can act as antibacterial reported by previous literature. The bonding between the film and the negatively charged bacteria results in electrostatic interactions and the activity of ZnO or CuO nanoparticles through photocatalytic activity can contribute to enhancing the antibacterial effect [47]. Akintelu and Folorunso [59] reported that the reactive oxygen species (ROS) and the particle size of ZnO and CuO nanoparticles also can contribute to the antibacterial effect. The

release of Cu^{2+} and Zn^{2+} ions and their interaction with the negatively charged cell of bacteria may also enhance antibacterial [60]. The effect of the release of Zn^{2+} ions, followed by reactive oxygen species such as OH^\cdot , H_2O_2 , also O_2^{2-} [61], and the difference of ionic radius between Cu^{2+} and Zn^{2+} ions can enhance antibacterial activity because the effect of crystallite size [62].

CONCLUSION

ZnO , CuO , and ZnO/CuO nanoparticles can be biosynthesized successfully using the ethanolic extract of guava seed leaves as a medium. The synthesis of films A-E requires ZnO , CuO , and ZnO/CuO nanoparticles. The Zn-O and Cu-O groups can be observed in the FTIR spectrum of ZnO/CuO nanoparticles and PVA-chitosan- ZnO/CuO nanoparticles. The physical structure of ZnO , CuO , and ZnO/CuO nanoparticles is crystalline, whereas the physical structure of the PVA-chitosan- ZnO/CuO nanoparticles film is amorphous. ZnO/CuO nanoparticles can change the surface morphology of chitosan in the PVA-chitosan- ZnO/CuO nanoparticles film. The antibacterial activity of film D is higher than C and E.

ACKNOWLEDGEMENT

This research was funded by Sekolah Tinggi Ilmu Farmasi Bhakti Pertiwi and we are thankful for STIFI Bhakti Pertiwi.

REFERENCES

- [1] A.N. Ul Haq, A. Nadhman, I. Ullah, G.M. Mustafa, M. Yasinzai, and I. Khan, "Review article synthesis approaches of zinc oxide nanoparticles: The dilemma of ecotoxicity". *Hindawi J. Nanomater.*, **2017**(12), 1-14, 2017, doi: 10.1155/2017/8510342.
- [2] K. Bloch, K. Pardesi, C. Satriano, and S. Ghosh, "Bacteriogenic platinum nanoparticles for application in nanomedicine", *Front. Chem.*, **9**, 624344, 2021, doi: 10.3389/fchem.2021.624344.
- [3] D. Zhang, X.I. Ma, Y. Gu, H. Huang, and G.W. Zhang, "Green synthesis of metallic nanoparticles and their potential applications to treat cancer", *Front. Chem.*, **8**, 799, 2020, doi: 10.3389/fchem.2020.00799.
- [4] N. Pantidos, and L.E. Horsfall, "Biological synthesis of metallic nanoparticles by bacteria, fungi and plants". *J. Nanomed.Nanotechnol.*, **5**, 233, 2014, doi: 10.4172/2157-7439.1000233.
- [5] D. Letchumanan, S.P.M. Sok, S. Ibrahim, N.H. Nagoor, and N.M. Arshad, "Plant-based biosynthesis of copper/copper oxide nanoparticles: An update on their applications in biomedicine, mechanisms, and toxicity", *Biomolecules*, **11**(4), 564, 2021, doi: 10.3390/biom11040564.
- [6] B.N. Singh, A.K.S. Rawat, W. Khan, A.H. Naqvi, and B.R. Singh, "Biosynthesis of stable antioxidant ZnO Nanoparticles by *Pseudomonas aeruginosa* Rhamnolipids", *PLoS ONE*, **9**(9), e106937, 2014, doi: 10.1371/journal.pone.0106937.
- [7] V.N. Kalpana, B.A.S. Kataru, N. Sravani, T. Vigneshwari, A. Panneerselvam, and D. Rajeswari, "Biosynthesis of zinc oxide nanoparticles using culture filtrates of *Aspergillus niger*: Antimicrobial textiles and dye degradation studies", *OpenNano*, **3**, 48-55, 2018, doi: 10.1016/j.onano.2018.06.001.
- [8] K. Lingaraju, H.R. Naika, K. Manjunath, R.B. Basavaraj, H. Nagabhushana, G. Nagaraju, and D. Suresh, "Biogenic synthesis of zinc oxide nanoparticles using *Ruta graveolens* (L.) and their antibacterial and antioxidant activities", *Appl. Nanosci.*, **6**, 703-710, 2016, doi: 10.1007/s13204-015-0487-6.
- [9] F.A. Jan, R. Wajidullah, N. Ullah, U. Ullah, S. Salman, and M. Usman, "Exploring the environmental and potential therapeutic applications of *Myrtus communis* L. assisted synthesized zinc oxide (ZnO) and iron doped zinc oxide (Fe-ZnO) nanoparticles", *J. Saudi Chem. Soc.*, **25**(7), 101278, 2021, doi: 10.1016/j.jscs.2021.101278.
- [10] A. Fatoni, M.A. Afrizal, A.A., Rasyad, and N. Hidayati, "ZnO nanoparticles and its interaction with chitosan: Profile spectra and their activity against bacterial", *JKPK*, **6**(2), 216-227, 2021, doi: 10.20961/jkpk.v6i2.48000.
- [11] P. Khandel, R.K. Yadaw, D.K. Soni, L. Kanwar, and S.K. Shahi, "Biogenesis of metal nanoparticles and their pharmacological applications: present status and application prospects", *J.*

- Nanostructure Chem.*, **8**, 217–254, 2018, doi: 10.1007/s40097-018-0267-4.
- [12] N. Muhamad, N.A. Muhmed, M.M. Yusoff, and J. Gimbut, “Influence of solvent polarity and conditions on extraction of antioxidant, flavonoids and phenolic content from *Averrhoa bilimbi*”, *J. Food Sci. Eng.*, **4**, 255-260, 2014, doi: 10.17265/2159-5828/2014.05.006
- [13] J.B. Harborne, I. Sudiro, K. Padmawinata, dan S. Niksolihin, “*Metode fitokimia: penuntun cara modern menganalisis tumbuhan*”. Bandung: Penerbit ITB, 2005.
- [14] S. Alamdari, M.S., Ghamsari, C. Lee, W. Han, H.H. Park, M.J. Tafreshi, H. Afarideh, and M.H.H. Ara, “Preparation and characterization of zinc oxide nanoparticles using leaf extract of *Sambucus ebulus*”, *Appl. Sci.*, **10**(10), 3620, 2020, doi: 10.3390/app10103620.
- [15] V.S. Chinni, S.C.B. Gopinath, P. Anbu, N.K. Fuloria, S. Fuloria, P. Mariappan, K. Krusnamurthy, L.V. Reddy, G. Ramachawolran, S. Sreeramanan, and S. Samuggam, “Characterization and antibacterial response of silver nanoparticles biosynthesized using an ethanolic extract of coccinia indica leaves”, *Crystals*, **11**(2), 97, 2021, doi: 10.3390/cryst11020097.
- [16] I. Fatimah, “Biosynthesis and characterization of ZnO nanoparticles using rice bran extract as low-cost templating agent”, *J. Eng. Sci. Technol.*, **13**(2), 409–420, 2018.
- [17] A. Fatoni, R.A. Sriwijaya, U. Habiba, and N. Hidayati, “CuO nanoparticles: biosynthesis, characterization and in vitro study”, *Sci. Technol. Indones*, **6**(1), 25–29, 2021, doi: 10.26554/sti.2021.6.1.25-29.
- [18] A. Fouda, S.S. Salem, A.R. Wassel, M.F. Hamza, and T.I. Shaheen, “Optimization of green biosynthesized visible light active CuO/ZnO nano-photocatalysts for the degradation of organic methylene blue dye”, *Heliyon*, **6**(9), e04896, 2020, doi: 10.1016/j.heliyon.2020.e04896.
- [19] J.O. Adeyemi, D.C. Onwudiwe, and A.O. Oyede, “Biogenic synthesis of CuO, ZnO, and CuO–ZnO nanoparticles using leaf extracts of *Dovyalis caffra* and their biological properties”, *Molecules*, **27**(10), 3206, 2022, doi: 10.3390/molecules27103206.
- [20] Y. Cao, H.A. Dhahad, M.A. El-Shorbagy, H. Q. Alijani, M. Zakeri, A. Heydari, E.M. Bahonar, M. Slouf, M. Khatami, M. Naderifar, S. Iravani, S. Khatami, and F.F. Dehkordi, “Green synthesis of bimetallic ZnO–CuO nanoparticles and their cytotoxicity properties”, *Sci. Rep.*, **11**, 23479, 2021, doi: 10.1038/s41598-021-02937-1.
- [21] D. Saravanakumar, S. Sivaranjani, K. Kaviyarasu, A. Ayeshamariam, B. Ravikumar, S. Pandiarajan, C. Veeralakshmi, M. Jayachandran, and M. Maaza, “Synthesis and characterization of ZnO–CuO nanocomposites powder by modified perfume spray pyrolysis method and its antimicrobial investigation”, *J. Semicond.*, **39**(3), 033001-1-7, 2018, doi: 10.1088/1674-4926/39/3/032001.
- [22] G. Sharma, A. Kumar, S. Sharma, M. Naushad, R.P. Dwivedi, Z.A. AlOthman, and G.T. Mola, “Novel development of nanoparticles to bimetallic nanoparticles and their composites: A review”, *J. King Saud Univ. Sci.*, **31**, 257–269, 2019, doi: 10.1016/j.jksus.2017.06.012.
- [23] S.A. Agnihotri, N.N. Mallikarjuna, and T.M. Aminabhavi, “Recent advances on chitosan-based micro- and nanoparticles in drug delivery”, *J. Controll. Release.*, **100**, (1), 5–28, 2004, doi: 10.1016/j.jconrel.2004.08.010
- [24] S.K. Kim, and N. Rajapakse, “Enzymatic production and biological activities of chitosan oligosaccharides (COS): a review”, *Carbohydr. Polym.*, **62**(4), 357–368, 2005.
- [25] I. Aranaz, A.R. Alcántara, M.C. Civera, C. Arias, B. Elorza, A.H. Caballero, and N. Acosta, “Chitosan: an overview of its properties and applications”, *Polymers*, **13**(19), 3256, 2021, doi: 10.3390/polym13193256.
- [26] A.M. Abdullah, S.B. Aziz, and S.R. Saeed, “Structural and electrical properties of polyvinyl alcohol (PVA): Methyl cellulose (MC) based solid polymer blend electrolytes inserted with sodium iodide (NaI) salt”, *Arab. J. Chem.*, **14**(103388), 2021, doi: 10.1016/j.arabjc.2021.103388.
- [27] T.A. Kareem, and A.A. Kaliani, “Synthesis and thermal study of octahedral silver nano-plates in polyvinyl alcohol (PVA)”, *Arab. J. Chem.*, **4**, 325–331, 2011, doi:10.1016/j.arabjc.2010.06.054

- [28] H. Isawi, "Using Zeolite/Polyvinyl alcohol/sodium alginate nanocomposite beads for removal of some heavy metals from wastewater", *Arab. J. Chem.*, **13**, 5691–5716, 2020, doi: 10.1016/j.arabjc.2020.04.009.
- [29] F. Croisier, and C. Jérôme, "Chitosan-based biomaterials for tissue engineering", *Eur. Polym. J.*, **49**, 780–792, 2013, doi: 10.1016/j.eurpolymj.2012.12.009.
- [30] H. Shawky, "Synthesis of ion-imprinting chitosan/PVA crosslinked membrane for selective removal of Ag(I)". *J. Appl. Polym. Sci.*, vol.114, no. 5, pp. 2608-2615, 2009, DOI:10.1002/app.30816
- [31] A. Kalia, M. Kaur, A. Shami, S.K. Jawandha, M.A. Alghuthaymi, A. Thakur, and K.A. Abd-Elsalam, "Nettle-leaf extract derived ZnO/CuO nanoparticle-biopolymer-based antioxidant and antimicrobial nanocomposite packaging films and their impact on extending the post-harvest shelf life of guava fruit", *Biomolecules*, **11**(2), 224, 2021, doi: 10.3390/biom11020224.
- [32] A. Fatoni, H.S. Yessica, A. Aldilah, M. Almi, A. Rendowaty, R. Romsiah, L. Sirumapea, and N. Hidayati, "The film of chitosan-ZnO nanoparticles-CTAB: synthesis, characterization and in vitro study", *Sci. Technol. Indones.*, **7**(1), 58-66, 2022, doi: 10.26554/sti.2022.7.1.58-66.
- [33] I. Isnaeni, E. Hendradi, and N.Z. Zettira, "Inhibitory effect of roselle aqueous extracts-HPMC 6000 gel on the growth of Staphylococcus aureus ATCC 25923", *Turk. J. Pharm. Sci.*, **17**(2), 190-196, 2020, doi: 10.4274/tjps.galenos.2019.88709.
- [34] L. Joseph, M. George, G. Singh, and P. Mathews, P. "Phytochemical investigation on various parts of *Psidium guajava*", *Ann. Plant Sci.*, **5**(2), 1265-1268, 2016, doi: 10.21746/aps.2016.02.001.
- [35] M.M.H. Khalil, E.H., Ismail, K.Z. El-Baghdady, and D. Mohamed, "Green synthesis of silver nanoparticles using olive leaf extract and its antibacterial activity", *Arab. J. Chem.* **7**, 1131-1139, 2014, doi: 10.1016/j.arabjc.2013.04.007.
- [36] P.G. Bhavyasree, and T. S. Xavier, "Green synthesis of copper oxide/carbon nanocomposites using the leaf extract of adhatoda vasica nees, their characterization and antimicrobial activity", *Heliyon*, **6**, e03323, 2020, doi: 10.1016/j.heliyon.2020.e03323.
- [37] A.E.D. Mahmoud, K.M. Al-Qahtani, S.O. Alflajj, S.F. Al-Qahtani, and F.A. Alsamhan, "Green copper oxide nanoparticles for lead, nickel, and cadmium removal from contaminated water", *Sci. Rep.*, **11**(1), 12547, 2021, doi: 10.1038/s41598-021-91093-7.
- [38] M. Pandey, M. Singh, K. Wasnik, S. Gupta, S. Patra, P.S. Gupta, D. Pareek, N.S.N. Chaitanya, S. Maity, A.B.M. Reddy, R. Tilak, and P Paik, "Argeted and enhanced antimicrobial inhibition of mesoporous ZnO–Ag₂O/Ag, ZnO–CuO, and ZnO–SnO₂ composite nanoparticles", *ACS Omega*, **6**, 31615–31631, 2021.
- [39] N. Matinise, X.G. Fuku, K. Kaviyarasu, N. Mayedwa, and M. Maaza, "ZnO nanoparticles via Moringa oleifera green synthesis: Physical properties & mechanism of formation", *Appl. Surf. Sci.*, **406**, 339–347, 2017, doi: 10.1016/j.apsusc.2017.01.219.
- [40] H. Hemalatha, and M. Makeswari, "Green synthesis, characterization and antibacterial studies of CuO nanoparticles from eichhornia crassipes", *Rasayan J. Chem.* **10**(3), 838-843, 2017, doi: 10.7324/RJC.2017.1031800.
- [41] D. Berra, S. Laouini, B. Benhaoua, M. Ouahrani, D. Berrani, and A. Rahal, "Green synthesis of copper oxide nanoparticles by *Pheonix dactylifera* L. leaves extract", *Dig. J. Nanomat. Biostructures.*, **13**(4), 1231–1238, 2018.
- [42] M. Altikatoglu, A. Attar, F. Erci, C.M. Cristache, and I. Isildak, "Green synthesis of copper oxide nanoparticles using *Ocimum basilicum* extract and their antibacterial activity", *Fresenius Environ. Bull.*, **25**(12), 7832–7837, 2017.
- [43] R. Dobrucka, and J. Dugaszewska, "Biosynthesis and antibacterial activity of ZnO nanoparticles using Trifolium pratense flower extract", *Saudi J. Biol. Sci.*, **23**, 517–523, 2016, doi: 10.1016/j.sjbs.2015.05.016.
- [44] S.S. Mydeen, R.R. Kumar, M. Kottaisamy, and V.S. Vasantha, "Biosynthesis of ZnO nanoparticles through extract from Prosopis juliflora plant leaf: Antibacterial activities and a new approach by rust-induced photocatalysis", *J. Saudi Chem.*

- Soc.*, **24**(5), 393-406, 2020, doi: 10.1016/j.jscs.2020.03.003.
- [45] M.A. Norouzi, M. Montazer, T. Harifi, and P. Karimi, "Flower buds like PVA/ZnO composite nanofibers assembly: Antibacterial, in vivo wound healing, cytotoxicity and histological studies", *Polym. Test.*, **93**, 106914, 2021, doi: 10.1016/j.polymertesting.2020.106914.
- [46] S. Kumaraswamy, G. Babaladimath, V. Badalamoole, and S. H. Mallaiah, "Gamma irradiation synthesis and in vitro drug release studies of ZnO/PVA hydrogel nanocomposites", *Adv. Mater. Lett.*, **8**(4), 546-552, 2017, doi: 10.5185/amlett.2017.6819.
- [47] R.A. Krishnan, O. Mhatre, J. Sheth, S. Prabhu, R. Jain, and P. Dandekar, "Synthesis of zinc oxide nanostructures using orange peel oil for fabricating chitosan-zinc oxide composite films and their antibacterial activity", *J. Polym. Res.*, **27**, 206, 2020, doi: 10.1007/s10965-020-2033-9.
- [48] A. Annu, A. Akbar, and S. Ahmed, "Eco-friendly natural extract loaded antioxidative chitosan/polyvinyl alcohol based active films for food packaging", *Heliyon*, **7**, e06550, 2021, doi: 10.1016/j.heliyon.2021.e06550.
- [49] D.S. Vicentini, A. Smania Jr, and M.C.M. Laranjeira, "Chitosan/poly (vinyl alcohol) films containing ZnO nanoparticles and plasticizers", *Mater. Sci.Eng. C.*, **30**, 503–508, 2010, doi:10.1016/j.msec.2009.01.026.
- [50] E. Prokhorov, G.L. Bárcenas, J.M.Y. Limón, A.G. Sánchez, and Y. Kovalenko, "Chitosan-ZnO nanocomposites assessed by dielectric, mechanical, and piezoelectric properties", *Polymers*, **12**(9), 1991, 2020, doi:10.3390/polym12091991.
- [51] K.S. Castillo, D.D.A.Lopez, A. M.T. Huerta, M.A.D. Crespo, D.P. Rami´rez, H. Willcock, and S.B.B. Sibaja, "Effect on the processability, structure and mechanical properties of highly dispersed in situ ZnO:CS nanoparticles into PVA electrospun fibers", *J. Mater. Res. Technol.*, **11**, 929-945, 2021.
- [52] K. Nithyaa, and S. Kalyanasundharam, S. "Effect of chemically synthesis compared to biosynthesized ZnO nanoparticles using aqueous extract of *C. halicacabum* and their antibacterial activity", *OpenNano*, **4**, 100024, 2019, doi: 10.1016/j.onano.2018.10.001.
- [53] H.C.A. Murthy, T.D. Zeleke, K.B. Tan, S. Ghotekar, M.W. Alam, R. Balachandran, K.Y. Chan, P.F. Sanaula, M.R.A. Kumar, and C.R. Ravikumar, "Enhanced multifunctionality of CuO nanoparticles synthesized using aqueous leaf extract of *Vernonia amygdalina* plant", *Results Chem.*, **3**, 100141, 2021, doi: 10.1016/j.rechem.2021.100141
- [54] A. Chinnathambi, and T.A. Alahmadi, "Zinc nanoparticles green-synthesized by *Alhagi maurorum* leaf aqueous extract: Chemical characterization and cytotoxicity, antioxidant, and anti-osteosarcoma effects", *Arab. J. Chem.* **14**, 103083, 2021, doi: 10.1016/j.arabjc.2021.103083.
- [55] S. Logpriya, V. Bhuvaneshwari, D. Vaidehi, R.P.S. Kumar, R.S.N. Malar, B.P. Sheetal, R. Asmaveni, and M. Kalaiselvi, "Preparation and characterization of ascorbic acid-mediated chitosan–copper oxide nanocomposite for anti-microbial, sporicidal and biofilm-inhibitory activity", *J. Nanostruct. Chem.*, **8**, 301–309, 2018, doi: 10.1007/s40097-018-0273-6.
- [56] C. Leonardelli, W.P. Silvestre, and C. Baldasso, "Effect of chitosan addition in whey-based biodegradable film", *Braz. Arch. Biol. Technol.*, **63**(6), e20200178, 2020, doi: 10.1590/1678-4324-2020200178
- [57] E. Susilowati, S.R.D. Ariani, L. Mahardiani, and L. Izzati, "Synthesis and characterization chitosan film with silver nanoparticle addition as a multiresistant antibacterial material", *JKPK.*, **6**(3), 371-383, 2021, <https://jurnal.uns.ac.id/jkpk>.
- [58] R.C. Goy, D. de Britto, and O.B.G. Assis, "A review of the antimicrobial activity of chitosan", *Polímeros: Ciência e Tecnologia*, **19**(3), 241-247, 2009, doi: 10.1590/S0104-14282009000300013.
- [59] S.A. Akintelu, and A.S. Folorunso, "A review on green synthesis of zinc oxide nanoparticles using plant extracts and its biomedical applications". *Bionanoscience.*, **10**(6-s), 2020, doi: 10.1007/s12668-020-00774-6.
- [60] R. Dadi, R. Azouani, M. Traore, C. Mielcarek, and A. Kanaev, "Antibacterial activity of ZnO and CuO nanoparticles against gram positive and gram negative

- strains”, *Mater. Sci. Eng. C*, **104**, 109968, 2019, doi: 10.1016/j.msec.2019.109968.
- [61] G.K. Weldegebrieal, “Synthesis method, antibacterial and photocatalytic activity of ZnO nanoparticles for azo dyes in wastewater treatment: A review”, *Inorg. Chem. Commun.*, **120**, 108140, 2020, doi: 10.1016/j.inoche.2020.108140.
- [62] A. Al Baroot, M. Alheshibri, Q. A. Drmoh, S. Akhtar, E. Kotb, and K.A. Elsayed, “A novel approach for fabrication ZnO/CuO nanocomposite via laser ablation in liquid and its antibacterial activity”, *Arab. J. Chem.*, **15**(2), 103606, 2022, doi: 10.1016/j.arabjc.2021.103606.